Journal of Information Display
Vol. 12, No. 4, December 2011, 223–227

Taylor & Francis
Taylor & Francis Group

Solution-processed electrophosphorescent devices with a thin fluoropolymer at the hole transport interfacial layer

Jae Kyun Park[a], Gyoung Seok Hwang[a], Tae Woo Lee[b], and Byung Doo Chin[a]*

[a]*Department of Polymer Science and Engineering, Dankook University, Yongin 448-701, South Korea;* [b]*Department of Materials Science and Engineering, Pohang University of Science and Technology, Pohang 790-784, South Korea*

(*Received 15 August 2011; Revised 30 August 2011; Accepted 5 September 2011*)

Electrophosphorescent devices with ionomer-type hole transport layers were investigated. On top of the 3,4-ethylenedioxy thiophene:poly(4-styrene sulfonate) [PEDOT:PSS] structures, fluoropolymer interfacial layers (FPIs) with different side chain lengths were introduced. Both for the PEDOT:PSS/FPI (layered) and PEDOT:PSS (mixed) structures with soluble phosphorescent emitters, the short-side-chain FPIs showed higher efficiency. The difference in the electrical properties of the two FPIs for bipolar (light-emitting) devices was not clear, but the hole-only device clearly showed the favored hole injection at the PEDOT:PSS/FPI structure with a shorter side chain, a copolymer of tetrafluoroethylene and sulfonyl fluoride vinyl ether.

Keywords: electrophosphorescent, fluoropolymer, interfacial layer, soluble

1. Introduction

Organic light-emitting diodes (OLEDs) with solution-processed electrophosphorescent emitters (dispersed small-molecular dyes in a matrix of polymeric or small molecular hosts) have been widely investigated [1–3]. In addition to the development of efficient host/dopant light-emitting materials, the achievement of charge carrier balance through the engineering of interfacial layers is an important technique for the further enhancement of the solution OLEDs with electrophosphorescent emitters. As contact with PEDOT:PSS, a conventional hole injection layer for a soluble emitter-based OLED, has been known to be the main source of an unstable interface especially in phosphorescent devices, the use of an interfacial layer on top of a PEDOT:PSS structure or of a graded molecular profile for a PSS composite layer has been investigated [4–7]. Such modification presented a stepped electronic profile of the energy levels, leading to the realization of better hole injection control with a reduction of electron leakage. Energy-wise, however, the efficiency of the solution-processed phosphorescent OLEDs with low-triplet-energy interfacial layers, such as most of the conjugated polymers, must be reduced [8,9]. The slightly dissolved interfacial-layer material for the layer-by-layer coating can be the main reason for the significant quenching. Recently, a multilayer-structured soluble phosphorescent OLED with a controllable interface using hole transport and a light-emitting layer with cross-linkable small molecular elements was reported, showing efficiencies of up to 58 lm/W for green emission [10], even though there are still demands for the effective interfacial-layer materials for solution-based phosphorescent OLEDs.

In this study, fluoropolymer-type interfacial layers with different side chain lengths were employed to improve the performance of the soluble phosphorescent devices. Both for the evaporated and soluble-emitter-based devices, the OLED efficiency and current-voltage characteristics were compared at various interfacial-layer thicknesses and side chain lengths (type of fluoropolymer interfacial layer; hereafter, FPI). Along with the investigation of the device performance, the facilitated hole injection at the optimal interfacial-layer structure was examined by analyzing the hole-only-current characteristics. The comparison of the PEDOT:PSS/FPI (FPI thickness) and PEDOT:PSS-FPI mixture (concentration) provides a more detailed interpretation of the structure-property relationship of FPI-based phosphorescent devices.

2. Experiment

On a clean 4-mm^2 indium tin oxide (ITO) substrate with a sheet resistance of 15 Ohm/sq, PEDOT:PSS (Baytron P TP AI4083, H.C. Starck) was spin-coated and baked at 100°C in a nitrogen atmosphere for 30 min. Two fluoropolymers with different side chain lengths, Nafion™ (5.0 wt% in a mixture of lower aliphatic alcohols and water; Du Pont/Aldrich) and Aquivion™ (tetrafluoroethylene/sulfonyl fluoride vinyl ether; 6.0 wt% in a mixture of water/1-propanol/2-propanol; Solvey Solexis), were used for the fabrication of an ionomer-type interfacial layer. These materials,

*Corresponding author. E-mail: bdchin@dankook.ac.kr

ISSN 1598-0316 print/ISSN 2158-1606 online

http://dx.doi.org/10.1080/15980316.2011.622857
http://www.tandfonline.com

Table 1. Configuration of the FPIs of devices with evaporated phosphorescent emitters, and their light-emitting characteristics. Nafion^{TM}:methanol 1:10 and 1:15 solutions were used for the 5- and 10-nm-thick FPIs, respectively. The thickness of the Aquivion^{TM} layer was adjusted by varying the spin-coating rpm. Device structure: ITO/PEDOT:PSS/FPI/NPB/CBP:Ir(ppy)$_3$/BAlq/Alq$_3$/LiF/Al

Devices	PEDOT:PSS	FPI	Turn-on Voltage	Efficiency (cd/A)	Brightness (cd/m^2)
A1	AI4083 30 nm	×	3.1	19.7	1125 (5.0 V)
A2	AI4083 30 nm	Nafion^{TM} 5 nm	3.1	21.4	1447 (5.5 V)
A3	AI4083 30 nm	Nafion^{TM} 10 nm	3.2	23.6	1333 (6.5 V)
A4	AI4083 30 nm	Aquivion^{TM} 5 nm	3.1	21.4	1358 (6.0 V)
A5	AI4083 30 nm	Aquivion^{TM} 10 nm	3.2	26.8	1299 (6.0 V)

which have high proton conductivity and tunable electrical properties, are typically used as perfluorosulfonic-acid membranes in fuel cells. First, diluted dispersion of the FPIs (Nafion^{TM} and Aquivion^{TM}) was done, providing the solutions with an FPI:methanol ratio of 1:15, 1:10 (for Nafion^{TM}) and 1:20 (for Aquivion^{TM}). The device codes and thicknesses of the FPIs are listed in Table 1. After spin-coating, the FPIs were thermally annealed at 100°C in a nitrogen atmosphere for 30 min. The thicknesses of the spin-coated organic layers were measured with a surface profiler (Veeco Instruments). As the thickness of the interfacial layer (<10 nm) was hard to measure via the conventional profilometry, the difference between the thickness of the double layer (PEDOT:PSS/FPI) and that of the single PEDOT:PSS layer was measured.

In the case of an evaporation device, a phosphorescent light-emitting layer (30 nm; 4,4'-N,N'-dicarbazole-biphenyl [CBP] doped with 5% fac-Tris(2-phenylpyridine) iridium(III) [Ir(ppy)$_3$]) was deposited at a vacuum level of 2×10^{-7} Torr. The solution-processed phosphorescent emitter was a mixture of 4,4'-N,N'-dicarbazole-biphenyl (CBP), poly(9-vinyl carbazole) (PVK), and Ir(ppy)$_3$, with a weight ratio of 47.5:47.5:5 (toluene solution). The chemical structures of the phosphorescent light emitters and the FPIs are shown in Fig. 1. 5-nm-thick aluminum (III) bis(2-methyl-8-quinolinato)4-phenyl phenolate (BAlq; 5 nm) and tris(8-hydroxyquinoline) aluminum (Alq$_3$; 25 nm) were used as a hole blocker and as an electron-transporting layer, respectively. Lithium fluoride/Al cathode (100 nm) was employed. Device structures with evaporated or solution-processed emitters, and hole-only devices, are shown in Fig. 2 along with the materials' relevant energy levels. The evaluation of the highest-occupied-molecular-orbital (HOMO) level for the light-emitting layers (host/dopant) and NPB was performed with Riken-Keiki AC2. Cyclic voltammetry was employed to measure the ionization potentials (IPs) of the FPIs. The procedures of the analytical methods of the stacked thin film and surface chemical data (such as X-ray photoelectron spectroscopy in the case of Nafion^{TM}) are shown elsewhere [11]. The devices' luminance-current-voltage characteristics were measured with a source measurement unit (Keithley 2400) and Minolta CS-1000.

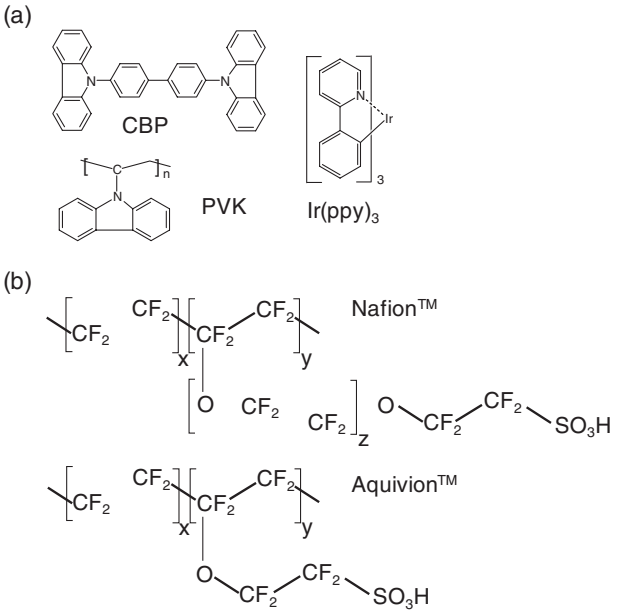

Figure 1. Materials that were employed for the light-emitting layers (a) and FPIs as hole injection promoters (b).

3. Results and Discussion

The plots of the current density vs. bias voltage and the efficiency behavior of the devices with evaporated phosphorescent emitters are shown in Fig. 3. The luminous efficiency (cd/A) of devices A2-A5 (with FPIs; see Table 1) is higher throughout the whole brightness range compared to that of the control device (A1). Efficiency enhancement was observed in the two types of FPIs, while the device with short-chain-length Aquivion^{TM} (10 nm, A5) showed the best efficiency. The maximum efficiency of device A5 at 1000-1500 cd/m^2 was 26.8 cd/A while control device A1 showed 19.7 cd/A efficiency at the comparable brightness level.

On the other hand, the current injection was not favorable under the conditions of devices A2–A5. The I–V characteristics of these bipolar devices were different from those of the unipolar (hole-only) devices, as shown in Fig. 4. Here, the carrier conduction (influenced by both injection and transport) of the hole-only

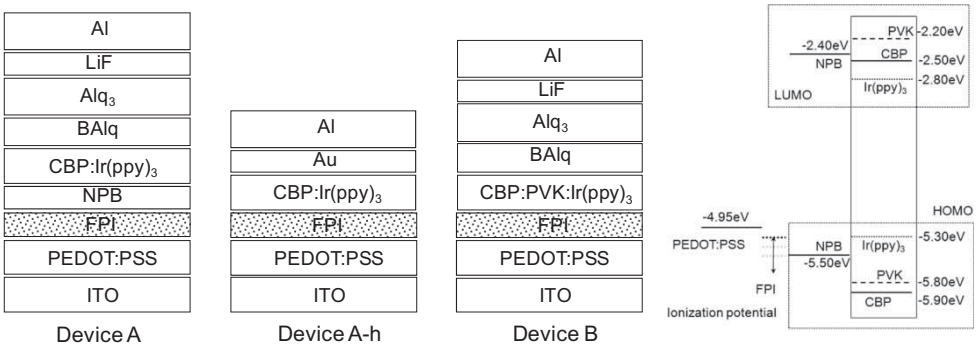

Figure 2. Device structures of A1–A5 (evaporated emitters), A1h–A5h (hole-only devices), and B1–B4 (soluble emitters) containing FPIs. The ionization potential, HOMO, and LUMO energy levels of the components of the hole-injecting and light-emitting layers (evaporated - CBP:Ir(ppy)$_3$; solution-processed - CBP:PVK:Ir(ppy)$_3$) are given.

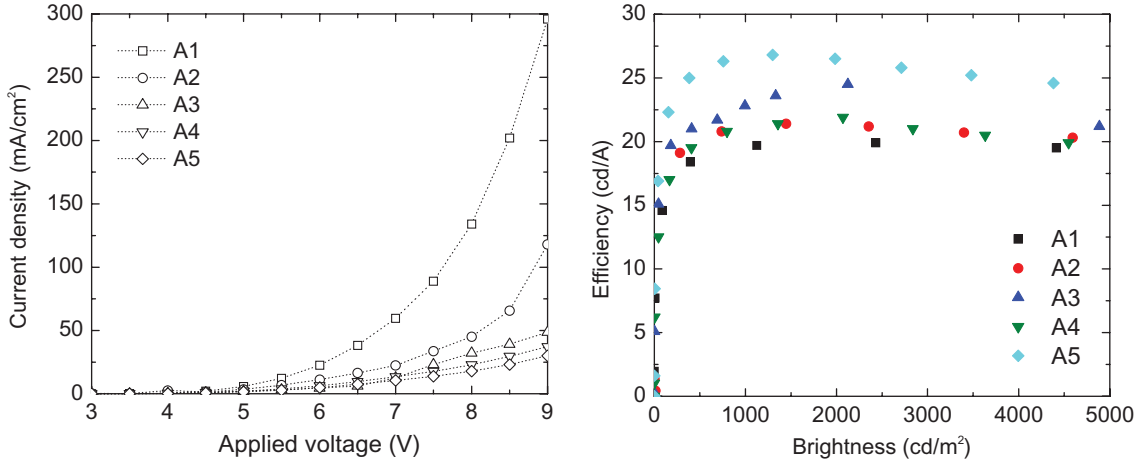

Figure 3. Current density vs. bias voltage (a) and luminous efficiency vs. brightness (b) of the phosphorescent devices with vacuum-evaporated emitters (30-nm-thick CBP:Ir(ppy)$_3$). The PEDOT:PSS/FPI configurations are given in Table 1.

devices (A1h–A5h) was investigated. The structure of the PEDOT:PSS/FPI layer in devices A1h–A5h (Fig. 4) was identical to that in devices A1–A5 (see Table 1). Hole-only devices with ITO/PEDOT:PSS (30 nm)/FPI (0, 5, or 10 nm)/CBP:Ir(ppy)$_3$ (30 nm)/Au (40 nm)/Al (60 nm) structures were fabricated for the Nafion^{TM}, Aquivion^{TM}, and control devices. Au cathode (work function: 5.4 eV) was used to block the electron injection through the lowest-unoccupied-molecular-orbital (LUMO) level of CBP (−2.5 eV). to the results of the IP measurement for the four samples via cyclic voltammetry (Table 3) clearly showed the tendency of a deeper (higher-absolute-value) IP level to increase the interfacial-layer thickness or the concentration of FPI at the PEDOT:PSS-FPI mixture, which is consistent with the other reports [6,11]. Therefore, the cascade HOMO level for a 10-nm-thick FPI structure can be the reason for the increase in the hole-only current. The apparent reduction of the hole injection barrier, as can be seen in Fig. 4, is more conspicuous at the FPI of Aquivion^{TM}. In the bipolar (light-emitting) device in Fig. 3, however, the holes injected from FPI to CBP:Ir(ppy)$_3$ are likely to fill the HOMO of Ir(ppy)$_3$. Therefore, not the lower hole injection barrier at PEDOT:PSS/FPI but the possible charge carrier traps at the interface of FPI (5/10 nm)/NPB (40 nm) are responsible for the lower current injection in the device data shown in Fig. 3. Reduction of the charge carrier trapping can be realized through the doping ration control or the proper engineering of the transport layers [12,13].

Based on the results of the density-functional theory calculations for the study on the ionization potentials and dipole moments of FPIs, it can be said that the fluorinated alkyl chain length does not significantly affect the IPs of the FPIs [6]. At a mixture of hydrocarbon sulfonic acids (such as PSS) and FPI, an increased concentration of FPI yields a deeper (far from vacuum) HOMO level. The increase of the thin FPIs on top of the PEDOT:PSS structure resulted in the same tendency [11]. The short-side-chain FPI (Aquivion^{TM}) has higher proton conductivity (147 S/cm) than Nafion^{TM} (101 S/cm), but the role of proton conductivity on the hole conduction or transport in the bipolar or unipolar diodes with an electronic process is not clear. The short-side-chain FPI (Aquition^{TM}, with a higher glass transition temperature of 126°C compared with Nafion^{TM}, which has 67°C) will at least provide better thermal stability

at the annealing process higher than 100°C, possibly having more stable contact at the layered structures.

Fig. 5 shows the current density vs. bias voltage and luminous efficiency vs. brightness for solution-processed green phosphorescent devices (B1–B5; see Table 2 for the specific device structures). Here, FPI's side chain length and the layered vs. mixed structure of the PEDOT:PSS-FPI system were proven. Both for the PEDOT:PSS/FPI (layered) and PEDOT:PSS (mixed) structures, the short-side-chain FPI (Aquition^{TM}) showed higher efficiency, as can be seen in Fig. 5b. Compared with the reference (B1; 17.3 cd/A at 7.5 V; 708 cd/m^2), device B3, which had a 10-nm-thick Aquivion^{TM} FPI, showed improved current efficiency and higher brightness (26.0 cd/A at 7.5 V; 1417 cd/m^2). Unlike the evaporated device sets, these soluble emitter devices [PEDOT:PSS/FPI/CBP:PVK:Ir(ppy)$_3$] may be simply influenced by the assisted hole injection at the PEDOT:PSS/FPI/emitter cascade structure. In the case of the device fabrication for B4 and B5, a PEDOT:PSS-FPI mixture (5:1) was prepared using the 5.0 wt% Nafion^{TM} solution and the 6.0 wt% Aquivion^{TM} solution, respectively. A 30-nm-thick PEDOT:PSS+FPI mixture layer was formed. Similar to the layered devices (B2 and B3), B5, which had a short-side-chain FPI, showed higher efficiency than B4, but the enhancement of its luminous efficiency and brightness was not as significant as that in devices B2–B3. The PEDOT:PSS-FPI mixture will provide a self-organized film [6,12], having a concentration gradient with a PSS-rich phase at the ITO interface and an FPI-rich phase at the upper film (the condition was characterized through the measurement of the water contact angle). The surfaces of Nafion^{TM} and Aquivion^{TM} provided 102.1 and 105.3°

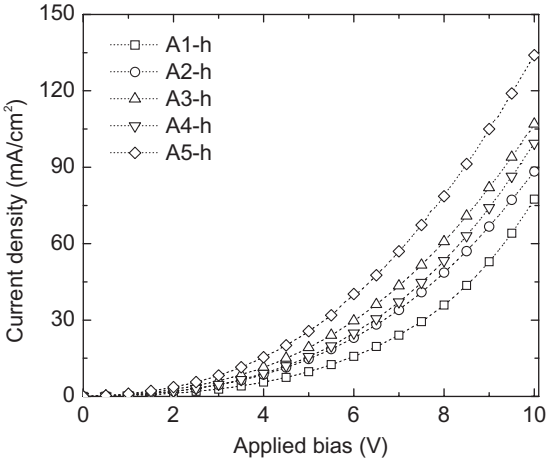

Figure 4. I–V characteristics of the hole-only devices (A1h–A5h) with the corresponding PEDOT:PSS/FPI configuration (A1–A5). The device structure is ITO/PEDOT:PSS/FPI/CBP:Ir(ppy)$_3$/Au/Al.

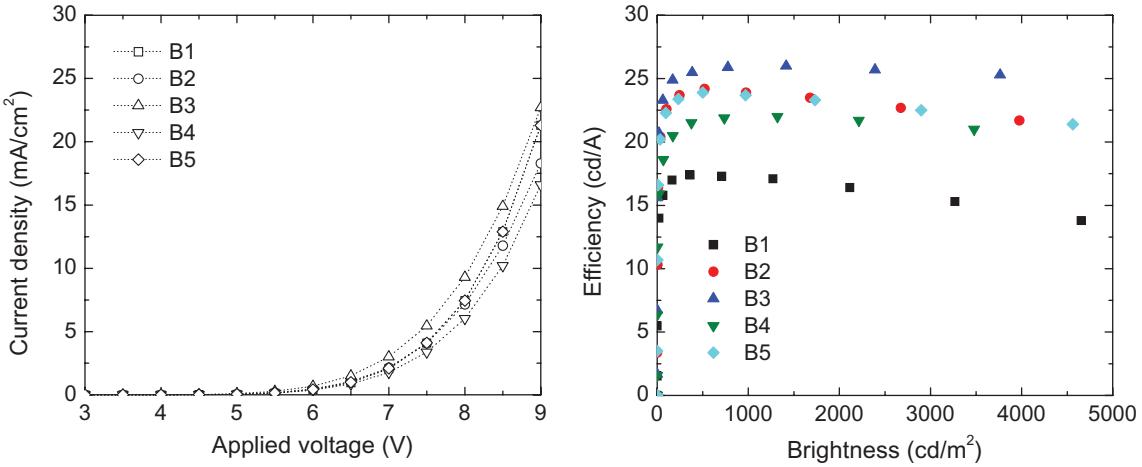

Figure 5. Current density vs. bias voltage (a) and luminous efficiency vs. brightness (b) of the phosphorescent devices with solution-processed emitters (30-nm-thick CBP:PVK:Ir(ppy)$_3$ blended). The PEDOT:PSS/FPI configurations are given in Table 2.

Table 2. Configuration of the FPIs of devices with solution-processed phosphorescent emitters, and their light-emitting characteristics. Device structure: ITO/PEDOT:PSS/FPI/CBP:PVK:Ir(ppy)$_3$/BAlq/Alq$_3$/LiF/Al (B2, B3) or ITO/PEDOT: PSS:FPI mixture/CBP:PVK:Ir(ppy)$_3$/BAlq/Alq$_3$/LiF/Al (B4, B5).

Devices	PEDOT:PSS	FPI	Turn-on Voltage	Efficiency (cd/A)	Brightness (cd/m^2)
B1	AI4083 30 nm	×	4.6	17.3	708 (7.5 V)
B2	AI4083 30 nm	Nafion^{TM} 10 nm	4.3	23.9	976 (7.5 V)
B3	AI4083 30 nm	Aquivion^{TM} 10 nm	4.3	26.0	1417 (7.5 V)
B4	AI4083:Nafion^{TM} Sol. (5:1) 30 nm	×	4.3	21.9	738 (7.5 V)
B4	AI4083:Aquivion^{TM} Sol. (5:1) 30 nm	×	4.3	23.7	971 (7.5 V)

Table 3. Ionization potentials of the PEDOT:PSS/FPIs or PEDOT:PSS-FPI mixtures for Aquivion^{TM} under various conditions.

Samples	Ionization Potential (by CV)
AI4083/Aquivion^{TM} 5 nm (layer)	5.43
AI4083/Aquivion^{TM} 10 nm (layer)	5.62
AI4083:Aquivion^{TM} 10:1 (mixture; 30 nm)	5.42
AI4083:Aquivion^{TM} 5:1 (mixture; 30 nm)	5.48

contact angles, respectively, while AI4083:Nafion^{TM} and AI4083:Aquivion^{TM} showed 79.6 and 85.3° contact angles, respectively. These values do not show a property as hydrophobic as that of pure FPI but one with a significantly higher value than that of pristine PEDOT:PSS (63°).

4. Summary

Fluoropolymer interfacial layers (FPIs) with different side chain lengths were compared for the evaluation of interfacial-layer-aided phosphorescent devices. The FPI with a short side chain length was more effective in the improvement of the luminous efficiency, while both FPIs posed the possibility of carrier trapping in the PEDOT:PSS/PFI/NBP/emitter structure. In the case of the soluble phosphorescent emitter structure (PEDOT:PSS/FPI emitter), a lower driving voltage and higher efficiency were achieved at the 10-nm-thick Aquivion^{TM}-containing device, yielding 26.0 cd/A at 7.5 V (1417 cd/m^2), while those of the control device remained at 17.3 cd/A at 7.5 V (708 cd/m^2). Therefore, in addition to the relative thickness or mixture composition of PSS:FPI, the type and properties of FPI are also important as design factors for soluble phosphorescent OLEDs. The issue of the competition between the injection barrier and interfacial charge trapping can be further validated by varying the host combination and adjacent supplementary transport layers.

Acknowledgements

This research was supported by the Basic Science Research Program through National Research Foundation of Korea (NRF) grants funded by the Ministry of Education, Science, and Technology (2009-0065638 and 2010-0010039).

References

[1] V. Cleave, G. Yahioglu, P. Le Barny, R. H. Friend, N. Tessler, *Adv. Mater. (Weinheim, Ger.)* **11**, 285 (1999).
[2] X. H. Yang, D. Neher, *Appl. Phys. Lett*. **84**, 2476 (2004).
[3] M.-H. Kim, M. C. Suh, J. H. Kwon, B. D. Chin, *Thin Solid Film*, **515**, 4011 (2007).
[4] P. K. H. Ho, J. S. Kim, J. H. Burroughes, H. Becker, S. F. Y. Li, T. M. Brown, F. Cacialli, R. H. Friend, *Nature* **404**, 481 (2000).
[5] P. K. H. Ho, M. Granström, R. H. Friend, N. C. Greenham, *Adv. Mater. (Weinheim, Ger.)* **10**, 769 (1998).
[6] T.-W. Lee, Y. Chung, O. Kwon, J.-J. Park, *Adv. Funct. Mater*. **17**, 390 (2007).
[7] M.-R. Choi, T.-H. Han, K.-G. Lim, S.-H. Woo, D. H. Huh, T.-W. Lee, *Angew. Chem. Int. Ed*. **50**, 1 (2011).
[8] M. Sudhakar, P. I. Djurovich, T. E. Hogen-Esch, M. E. Thompson, *J. Am. Chem. Soc.*, **125**, 7796 (2003).
[9] N. S. Kang, B.-K. Ju, J. W. Kim, J.-J. Kim, J.-W. Yu, B. D. Chin, *J. Appl. Phys*. **104**, 024511 (2008).
[10] . N. Rehmann, C. Ulbricht, A. Köhnen, P. Zacharias, M. C. Gather, D. Hertel, E. Holder, K. Meerholz, U. S. Schubert, *Adv. Mater. (Weinheim, Ger.)* **20**, 129 (2008).
[11] J. K. Park, G. S. Hwang, B. D. Chin, N. S. Kang, T.-W. Lee, Curr. Appl. Phys. (2011) doi:10.1016/j.cap.2011.04.030.
[12] W. S. Jeon, T. J. Park, J. H. Kwon, J. Information Display, **10**, 87 (2009).
[13] E. Böhm, R. Anemian, A. Büsing, R. Fortte, H. Heil, J. Kaiser, J. Kröber, S. Leu, T. Mujica-Fernaud, A. Parham, C. Pflumm & F. Voges, J. Information Display, **12**, 141(2011).
[14] M.-R. Choi, T.-H. Han, K.-G. Lim, S.-H. Woo, D. H. Huh, T.-W. Lee, Angew. Chem. Int. Ed. (2011) doi:10.1002/anie.201005031.